Limitations of WRF land surface models for simulating land use and land cover change in Sub-Saharan Africa and development of an improved model (CLM-AF v. 1.0)

Timothy Glotfelty, Diana Ramírez-Mejía, Jared Bowden, Adrian Ghilardi, and J. Jason West

Replies to Referee 1

Glotfelty et al. test the applicability of different LSMs incorporated in WRF RCM for Sub-Saharan Africa and their suitability to simulate the effects of land use changes on the regional climate conditions adequately. The results show that surface albedo, leaf area index and surface roughness are not accurately represented in the default models. Therefore, a new version of WRF coupled to the CLM LSM is developed, adjusted to the specific surface conditions in Sub-Saharan Africa. The topic of the study is within the scope of GMD and relevant for the large WRF modeling community in Africa and even beyond in the context of land use change effects on the regional climate in Africa. The manuscript is well structured and comprehensively written. The motivation of the paper is clear and the methods are well documented. Nevertheless, I have some concerns regarding the experimental setup, which need to be addressed by the authors before the manuscript is suitable for publication.

Response: We thank the reviewer for their comments on this work. Our point-by-point responses to the reviewer's comments can be found below.

Major comments:

1) In a first step, a model validation experiment is performed, in which simulations with five different models are conducted for one year. In general, I would say one year simulations are rather short to validate model performances, especially when only annual averages are presented. The authors argue that they chose the year 2013 because its a neutral year for the El Nino Southern Oscilation, but they do not really explain why this is the ideal boundary condition to validate the LSM performances. In any case, it is a single year that cannot represent the whole climate variability. Deviating atmospheric circulation conditions can considerably affect the impact of the land surface conditions on the regional climate conditions. Moreover, due to the exclusive consideration of annual averages, seasonal conditions are excluded in which the land surface conditions have larger impacts on the regional climate (e.g. dry conditions). Therefore, I recommend to extend the simulation period, or at least, to consider seasonal effects.

Response: We thank the reviewer for their comment. We understand the reviewer's concerns. The model validation experiment is meant to serve as an "out-of-the-box" meteorological comparison/evaluation of the WRF LSMs to illustrate the meteorological impacts of the default LSM deficiencies, rather than a full regional climate evaluation of the different model configurations. The rationale for this is that the WRF user community tends to use WRF in the "out-of-the-box" mode with minimal adjustments, for which the land cover/land use are

static and thus surface parameters are unchanging. To make this clearer, we have stated the proof-of-concept nature of our model evaluation more clearly in Section 4.1 and renamed the model validation experiment to the "meteorological evaluation experiment" (See below).

Lines 266-257 revised manuscript:

"The **meteorological evaluation** experiment consists of five simulations conducted for the year 2013, each using one of the five LSM configurations discussed above. The year 2013 is selected because it is a neutral year for the El Niño Southern Oscillation **(ENSO) and thus should be representative of the mean state of Sub-Saharan Africa's ENSO climate variability**. While a single year comparison does not yield climate relevant statistics, it is sufficient to demonstrate differences in the meteorology between the five LSM configurations and the mechanisms responsible for these differences. **This is because the prescribed surface parameters from the LSM do not vary between years and thus the impact from these parameters on the simulated meteorology will be similar (or at least the impact from each LSM will remain similar relative to the others) regardless of the model's overall meteorological state.** The **meteorological evaluation** simulations are conducted with default greenhouse gas concentrations and MODIS 21 class land use data. These default settings are chosen to illustrate the performance that can be expected from the publicly available WRF model."

Our overall goal with this experiment is to compare the impact of these surface parameters in different LSMs on the model's meteorological performance. Since the surface parameters do not vary between years within the WRF LSMs, the impact of the surface parameters from the LSMs will be similar relative to one another no matter which model year is simulated. For example, we find that the Noah LSM's albedo is strongly overestimated and this results in underpredicted surface temperatures. Therefore, no matter which meteorological years are simulated (i.e., whether that year is drier and less cloudy or moister and cloudier) the surface will always be too reflective and the surface energy balance will always be biased towards lower temperatures. While it is within the realm of possibility that in a particularly cold year the Noah LSM could perform better than the other LSMs, this would not be a meaningful result because the better agreement would be the result of an incorrect albedo. For these reasons, we do not think that extending the simulated period for the meteorological evaluation experiment would yield any more robust conclusions to justify the computational expense.

Per the reviewer's suggestion we have included seasonal surface plots in supplementary material (to save on space in the main text) to consider the seasonal evaluation of upwelling surface radiation at the Earth's surface (USRS), 2-m temperature (T2), and precipitation (See below). Additionally, references to these figures in the main text have been added (See bold and underlined below).

Lines 451-452 revised manuscript:

"Annual average spatial plots of USRS compared with CERES-EBAF estimates are shown in Fig. 7, **with seasonal average spatial plots shown in Fig. S5 of the supplementary material**."

Lines 468-459 revised manuscript:

"To understand the impact of surface parameters on near surface temperatures, the spatial plots of annual average T2 compared with CRU estimates are shown in Fig. 9, **with seasonal spatial plots shown in Fig. S10 of the supplementary material**."

Lines 507-508 revised manuscript:

"**Additionally, seasonal spatial plots of PRE compared with TRMM and annual average differences between TRMM and the LSMs and shown in Fig. S16 and Fig. S17, respectively**. All LSM simulations reasonably capture the annual (Fig. 11) **and seasonal (Fig. S16)** spatial patterns and magnitude of PRE."

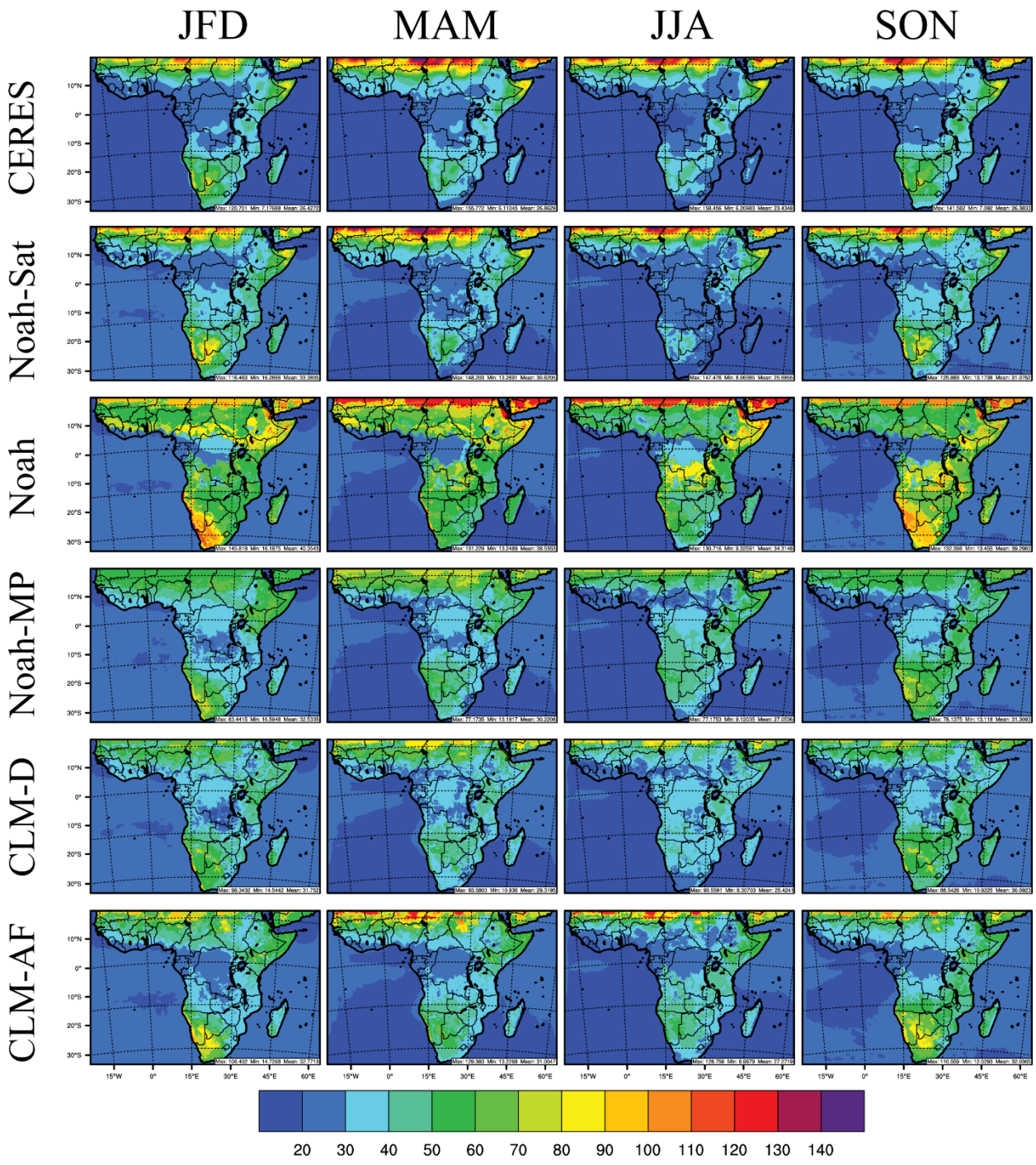

Fig S5: 2013 seasonal average upwelling shortwave radiation at the Earth's surface (W m^{-2}) for CERES-EBAF estimates and WRF

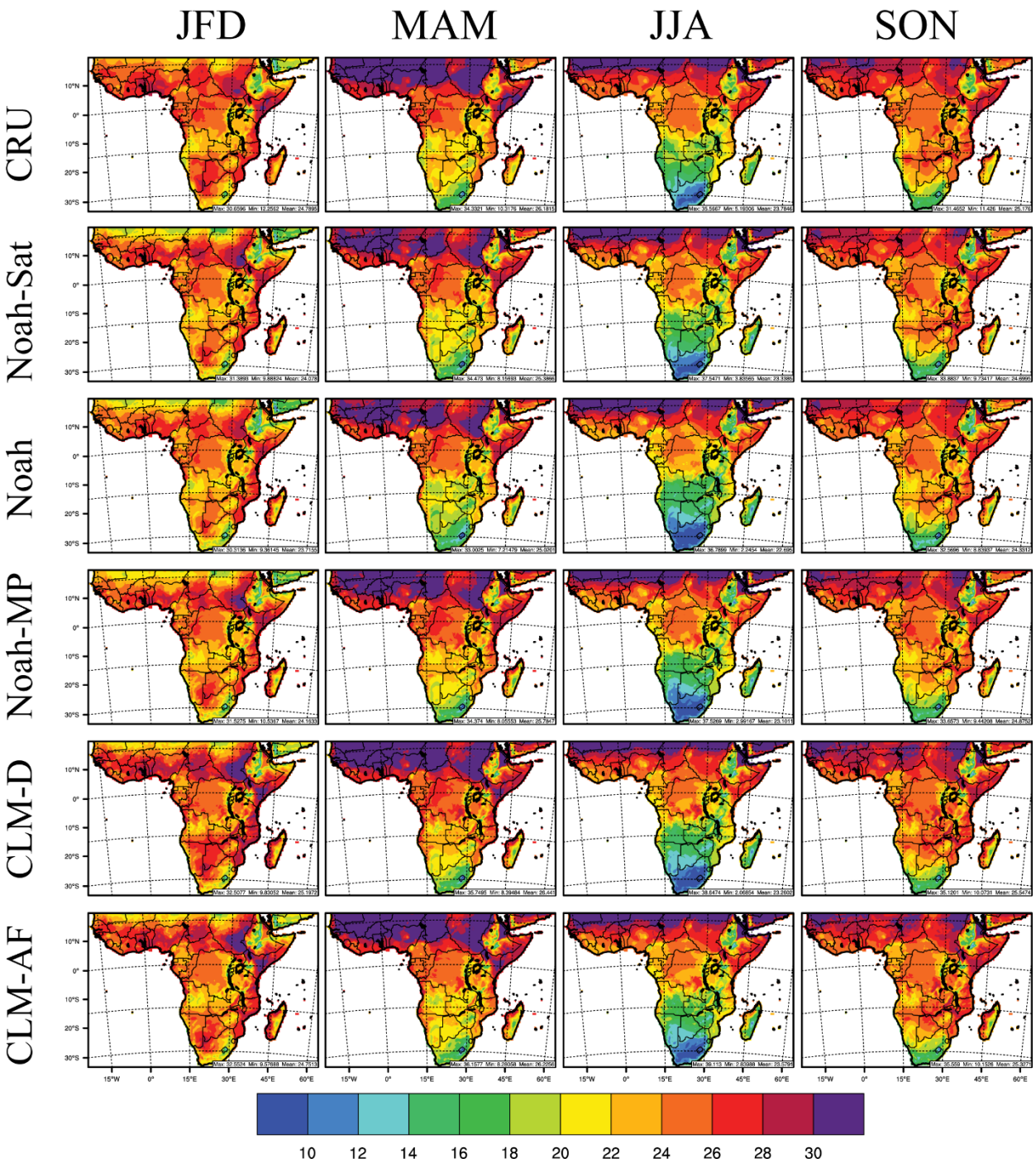

Fig S10: 2013 seasonal average 2-m temperature (°C) for CRU estimates and WRF

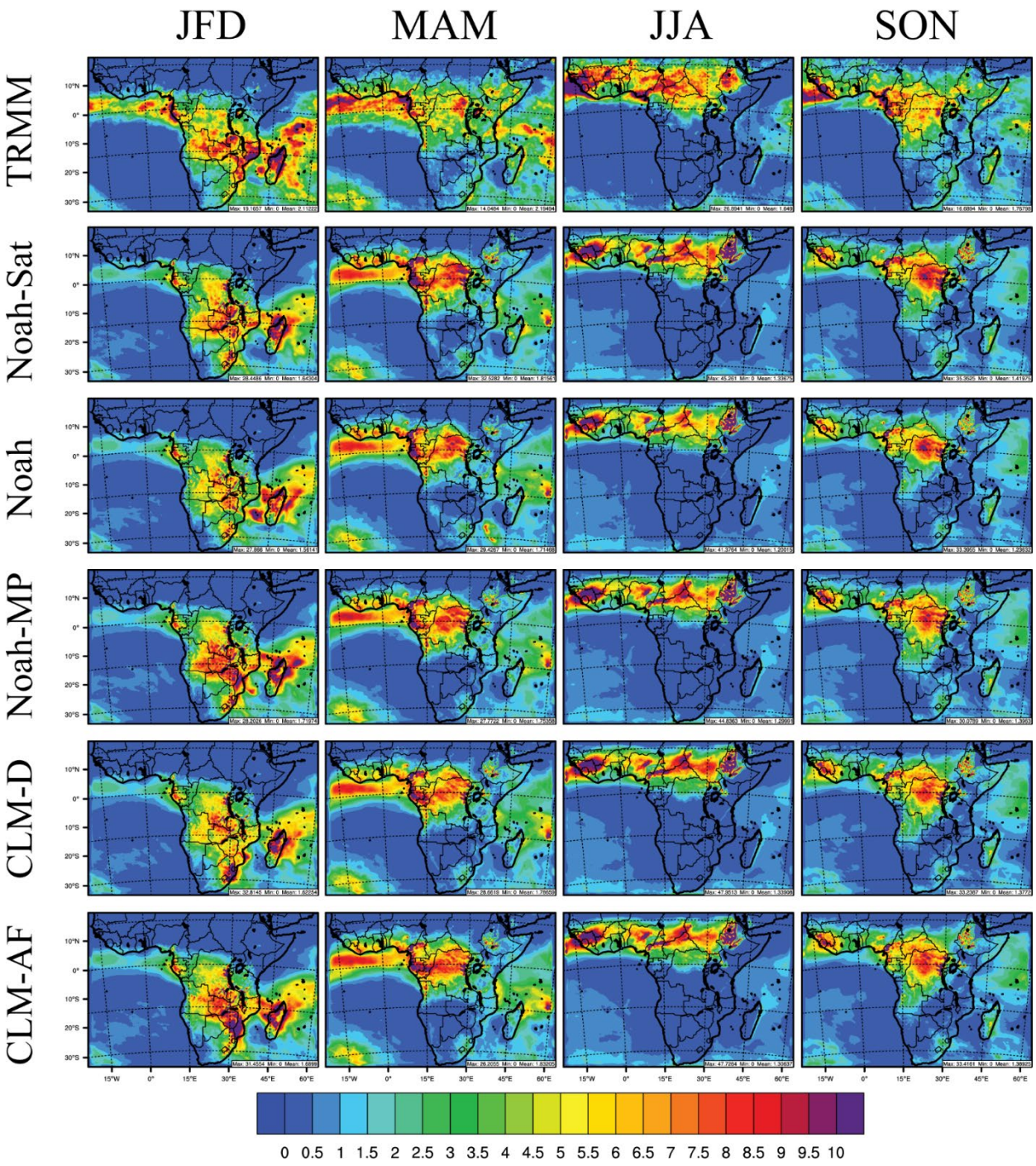

Fig S16: 2013 seasonal average precipitation (mm day^{-1}) for TRMM estimates and WRF

Based on the rationale mentioned above, the reason we chose an ENSO neutral year is because neutral/transition ENSO conditions are the most common (e.g., https://origin.cpc.ncep.noaa.gov/products/analysis_monitoring/ensostuff/ONI_v5.php) and thus this phase of the climate variability is the most representative of the mean state of Sub-Sahran Africa's ENSO climate variability. We have added this to the rationale in the main text (Lines 267-268 revised manuscript):

"**The year 2013 is selected because it is a neutral year for the El Niño Southern Oscillation and thus should be representative of the mean state of Sub-Saharan Africa's ENSO climate variability**".

2) In a second step, it is intended to quantify the impact of land use changes on the simulation results with different LSMs. For this, the results of climate simulations for the period 2001-2010 with static land use conditions are compared to results of climate simulations for the period 2010-2015, including observed land use changes. But differences between two simulations with different land use conditions do not have to be caused inevitably/exclusively by the different land use conditions, in the case of deviating simulation periods. The different atmospheric circulation conditions in both periods can have certain impacts on the simulation results. Thus, from my point of view, identical simulation periods would have been preferable (2001-2015). If it is not possible to perform these simulations with respect to computing time, one could eventually reduce the number of LSMs based on the results of the validation experiment. By the way, I do not really understand why Noah Sat is included in the study, if one cannot use it for land use change scenarios at all. The authors should at least discuss the potential effects of the different simulation periods.

Response: We thank the reviewer for their comment. There appears to be some confusion with regards to the land use impact experiments. In both simulations (i.e., LU01 and LUD) we are simulating the same six-year meteorological period of 2010 to 2015, we do not simulate the years 2001-2009 in either experiment. Therefore, the atmospheric circulation in both periods are identical as forced by the initial and boundary conditions, with the differences resulting only from the land use and land cover.

These simulations represent the effect of land use and land cover change since the year 2001. The LU01 simulations uses static LULC representing the year 2001 from MODIS but meteorology representative of the years 2010-2015, and the LUD experiment uses both LULC from Dinamica EGO and meteorology for the years 2010-2015.

Since understanding our simulation setup is critical, we have made significant revisions to improve how this is communicated (see underlined below).

Lines 277-291 revised manuscript:

"The LULCC experiment simulates **recent climate responses from LULCC since the year 2001 by comparing simulations with static LULC from 2001 with dynamic LULC representing 2010-2015. In both cases, meteorology is simulated for the six-year period of 2010-2015. These** two simulations differing in LULCC **are conducted for each LSM configuration, using the Noah, Noah-MP, CLM-D, and CLM-AF LSMs**. The first simulation for each LSM uses static LULC from **MODIS representing** the year 2001 for each simulated year (i.e., 2010-2015), hereafter referred to as LU01. The second uses dynamic LULC **from the MODIS 21 class land use dataset that is processed by the Dinamica EGO land use modeling framework (Soares-Filho et al., 2002 – described in more detail below)** for each simulated year **in the 2010-2015 period**, hereafter referred to as LUD. The **six-year average** differences between the LU01 and LUD simulations delineate the climate response to LULCC. **The time period 2010-2015 is selected because it is far enough away from the year 2001 to show significant impacts from LULCC and because it contains the full ENSO climate variability cycle.** Noah-Sat is excluded because LAI and albedo parameters derived from satellite data could be impacted by climatological variability**, and therefore do not only represent** LULCC. The LULCC simulations also utilize global average greenhouse gas concentrations for each simulation year **(2010-2015)** from the National Oceanic and Atmospheric Administration's (NOAA) Earth System Research Laboratory (ESRL) Global Monitoring Division. In the LULCC experiment, each year is a discreet simulation with a 3-month spin-up in which the model LULC is updated at the start of each year. This is necessary because the WRF modelling framework treats LULC as a static field."

As stated, it is difficult to use Noah-Sat to do a LULCC experiment, which is why it is not included in this second experiment (e.g., Figures 13-16). However, Noah-Sat is important for the meteorological evaluation experiment because it is the LSM configuration in WRF with the most accurate LAI and albedo parameters, which allows it to serve as a pseudo observation to compare the LSM parameters against. We have added this discussion to Section 2.1.1 in accordance with the suggestions of reviewer 2 (Lines 130-132 revised manuscript):

"**However, Noah-Sat is useful for meteorological evaluations, because it has the most accurate surface parameters in the current WRF modelling system. Therefore, Noah-Sat can be used as pseudo-observations to understand deficiencies in the surface parameter methodologies of the other WRF LSMs.**"

3) It is very difficult to assess the differences between the different LSMs in the validation experiment based on the shown figures. It is therefore very difficult to compare these differences to the changes caused by land use changes. Plots of the differences to observations as shown in section 7 would help a lot.

Response: We thank the reviewer for their comment. We evaluated model performance in the meteorological evaluation experiment through both soccer goal plots and spatial plots. The soccer goal plots provide insights into the model performance at both a domain-wide and regional level that convey to the reader how far off from the observations the different

parameters are. The spatial plots display how well the different model configurations capture the spatial patterns and magnitudes of our three key variables of interest (i.e., USRS, T2, and precipitation). Because we think these elements of the evaluation are the most relevant we have elected to keep these as the model evaluation figures in the main text. However, to assist readers and the reviewer we have also included difference plots of our three key variables in the supplementary material with citations in the main text (See below).

Lines 452-253 revised manuscript:

"**Additionally, annual average difference plots with CERES-EBAF for each LSM are shown in Fig. S6."**

Lines 469-470 revised manuscript:

"**Annual average differences between CRU and the LSMs are also shown in Fig. S11**."

Lines 472-473 revised manuscript:

"The only clear impact of surface albedo inaccuracy on annual average T2 is the relatively stronger cold bias in the Noah LSM (Fig. 9, **Fig. S11**)."

Lines 507-508 revised manuscript:

"**Additionally, seasonal spatial plots of PRE compared with TRMM and annual average differences between TRMM and the LSMs and shown in Fig. S16 and Fig. S17, respectively."**

Lines 510-512 revised manuscript:

"The greatest underpredictions occur in arid regions (ND, ED, SD, NESD, and WSD) and portions of East Africa (EM, CM, and LVW), while regions in South Africa (SSD and SM) and EW typically experience the strongest overprediction across the LSMs (Fig. 10, Fig. S12, **Fig. S17**)."

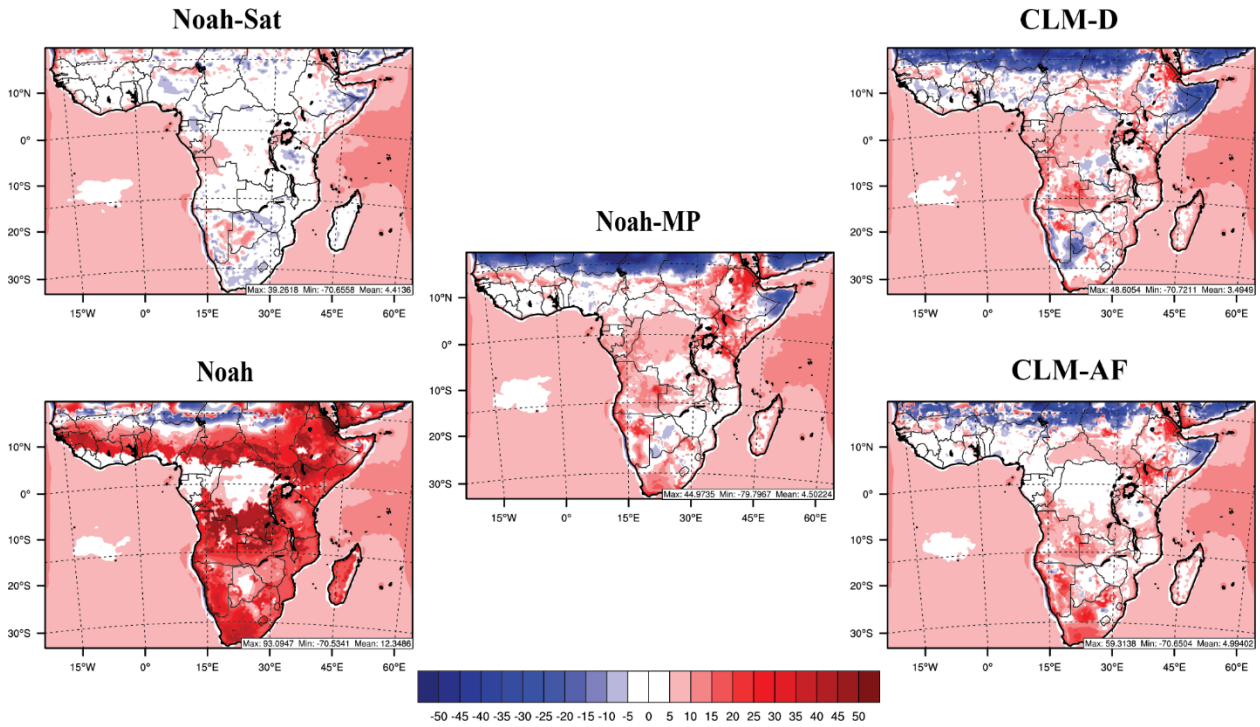

Fig S6: 2013 annual average differences in upwelling shortwave radiation at the Earth's surface (W m^{-2}) between the WRF simulations and CERES-EBAF estimates (WRF – CERES-EBAF)

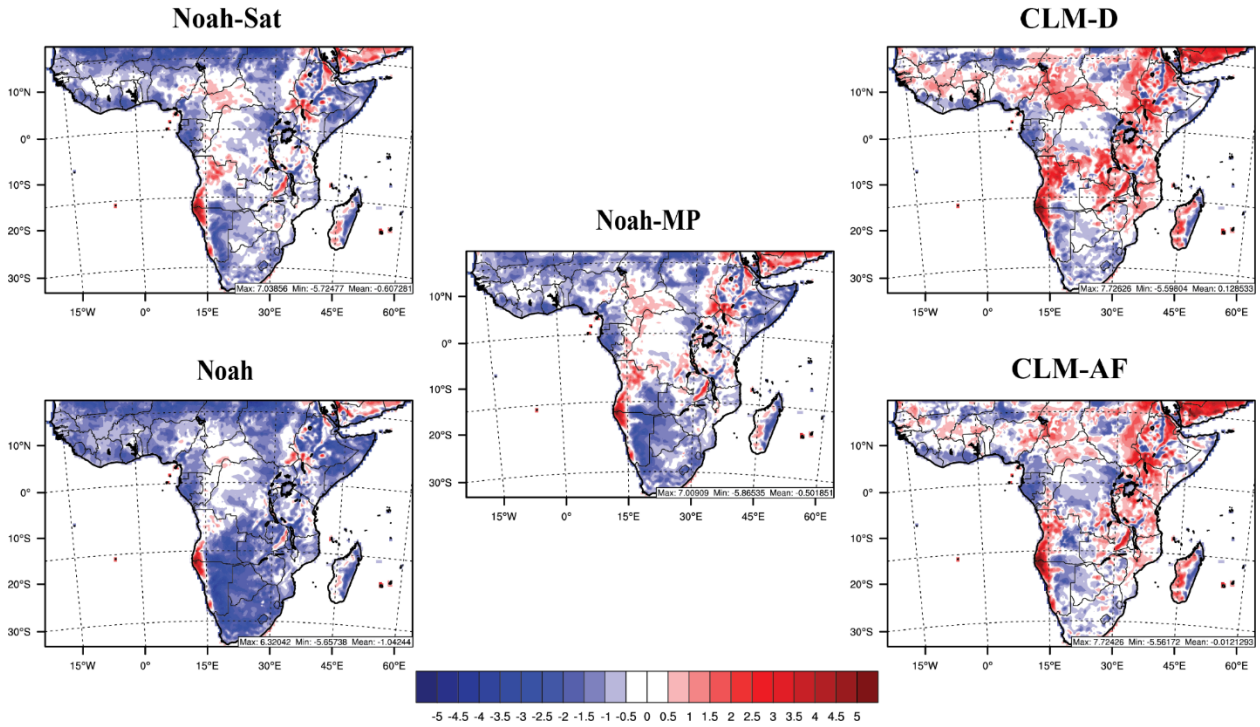

Fig S11: 2013 annual average differences in 2-m temperature (°C) between the WRF simulations and CRU estimates (WRF-CRU)

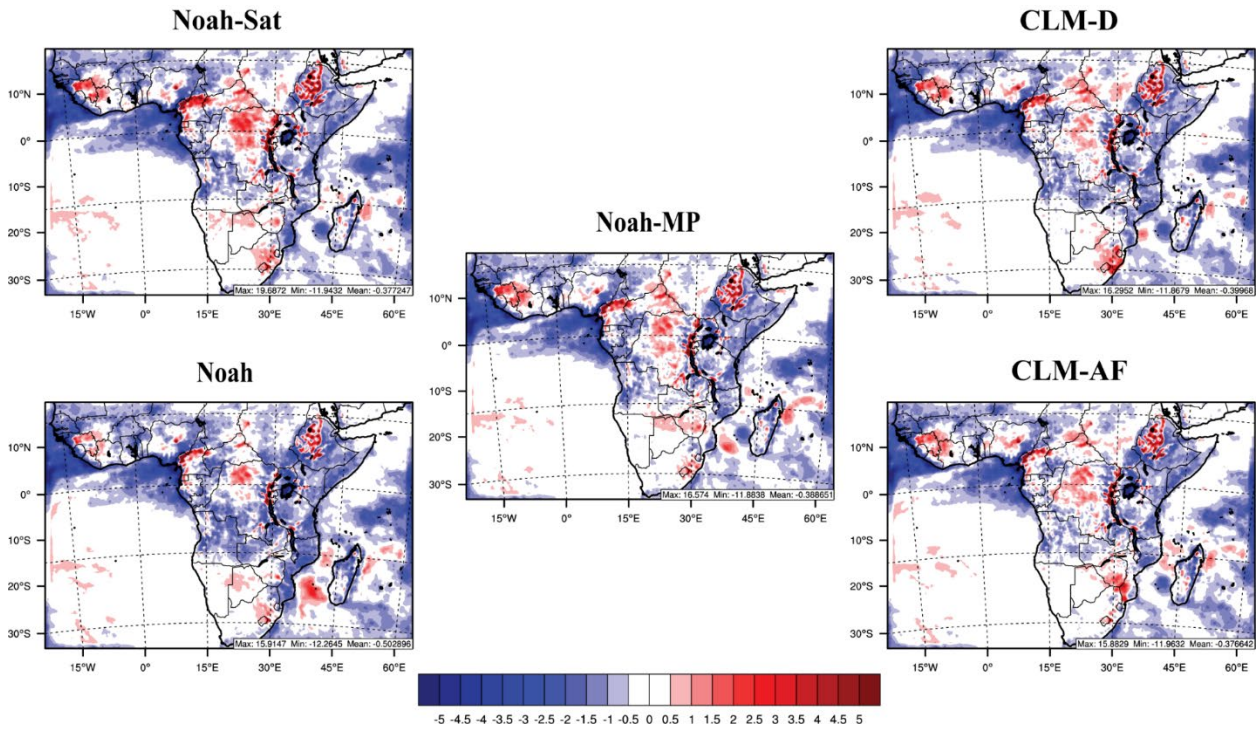

Fig S17: 2013 annual average differences in precipitation (mm day^{-1}) between the WRF simulations and TRMM estimates (WRF – TRMM)

4) To be able to understand the results of the validation experiment comprehensively, an assessment of the sensible and latent heat fluxes is necessary.

Response: We thank the reviewer for their comment. Per the reviewer's suggestion, we have included new Figures 5 and 6 that contain spatial plot comparisons of the annual average latent heat and sensible fluxes. Additionally, we have added the following discussion to the end of the results section 5 to discuss the differences in these parameters.

Lines 436-448 revised manuscript:

"For both latent (LH) and sensible (HFX) fluxes (Fig. 5 and Fig. 6), all LSMs produce similar annual average spatial distributions. LH are more similar amongst LSMs (Fig. 5), with the key difference being larger LH (~10–20 W m^{-2}) in the most heavily vegetated portions of the domain for the CLM-D and CLM-AF configurations. The similar LH for CLM-D and CLM-AF suggests a mechanistic difference that may be related to the vegetation canopy approximation in CLM that does not account for gaps within the canopy or between vegetation crowns. However, the values are the largest for CLM-AF in regions containing savanna, likely due to the larger values of LAI in these regions during the drier seasons (Fig. 3).

For HFX (Fig. 6), the Noat-Sat LSM produces the largest fluxes, especially in the semi-dry regions of eastern and southern Africa. This is likely a combination of Noah-Sat having the lowest albedo in vegetated regions leading to more surface energy absorption and Noah-Sat having consistently low LAI values in these regions throughout the year compared to other LSMs (Fig. 2 and Fig. 3). Both CLM-D and CLM-AF have lower HFX compared to the other

LSMs in vegetated areas, again likely due to the vegetation canopy assumptions. However, CLM-D has higher HFX in southern Africa comparable to those of Noah and Noah-MP. This is likely the result of Noah, Noah-MP, and CLM-D having much larger than realistic fluctuations in LAI between the wetter and drier seasons in this region (Fig. 3)"

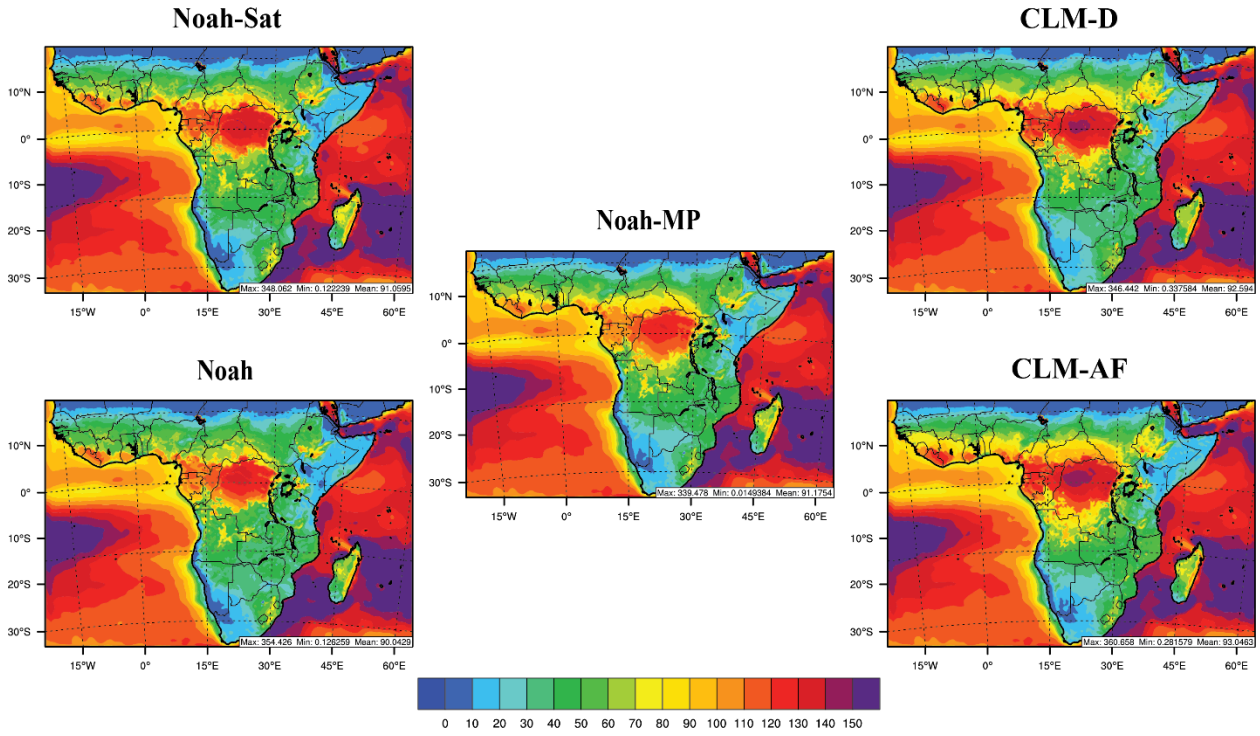

Figure 5: Comparison of annual average latent heat flux (W m^{-2}) between LSM configurations.

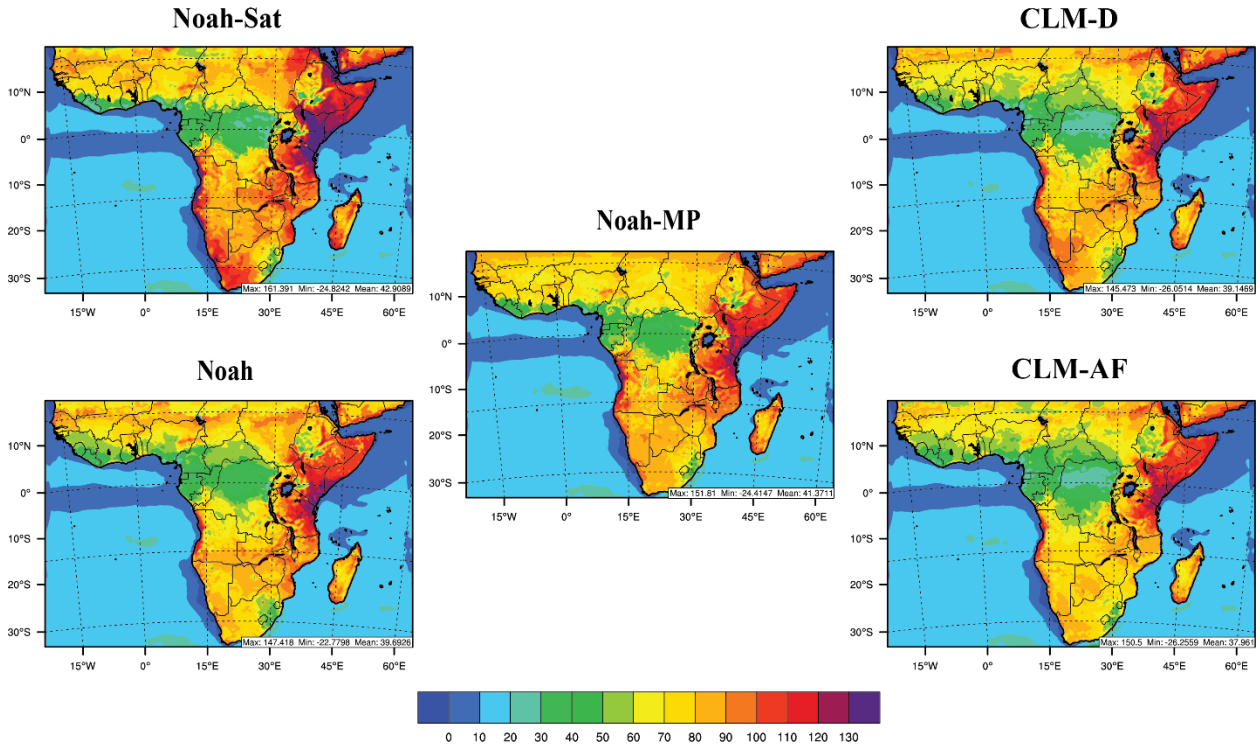

Figure 6: Comparison of annual average sensible heat flux (W m^{-2}) between LSM configurations.

Minor comments:

1) The biogeophysical effects of the surface roughness on the climate impacts of land use changes is not considered. For instance, this impact can be seen for the deforestation regions. The model results consistently show a warming with deforestation. In the manuscript, this is explained by reduced evapotranspiration rates and an associated reduced latent cooling. But if the reduced latent heat fluxes are the reason for the increased near-surface temperatures, accordingly the sensible heat fluxes should be increased (due to the increased temperature gradient between the land surface and the atmosphere). But this is not the case, the sensible heat fluxes are also reduced. Therefore, I suppose that the efficiency of the deforested land surface to transform the incoming solar energy in turbulent heat is reduced due to the reduced surface roughness, resulting in a warming of the surface (e.g. Winckler et al., 2019; Breil et al., 2020).

Response: We thank the reviewer for their comment, which provides a more complete explanation of the physical processes in the model. We have added several tables (S16-S27) in the supplementary material to include the full changes seen in the surface energy balance and near-surface temperature profiles. Additionally, we have made significant changes to Section 7.2 to account for the biogeophysical impacts of surface roughness length as shown below, and have revised the conclusions accordingly. However, even with the addition of this information it appears that the dominant factor controlling most of the warming and cooling predicted by the model is still increases or decreases in evaporative cooling.

Lines 579-658 revised manuscript:

"Changes in T2 between the LU01 and LUD simulations for each LSM are shown in Fig. 15. Locations that have the largest magnitude differences in T2 align with the more localized changes in LAI and albedo. Similar T2 patterns occur across the northern half of the domain when comparing Noah-MP, CLM-D, and CLM-AF simulations, while Noah predicts the most unique changes. To further investigate the LULCC impacts, **annual average** T2 differences are calculated for grid cells with different LULC transitions (see Table 10). **Additionally, we generate annual average differences of the surface energy budget and near surface temperature profiles for these grid cells, separately for daytime (SWDOWN > 0 W m^{-2}) and nighttime (SWDOWN = 0 W m^{-2}) conditions. The diurnally split radiative flux differences for USRS, SWDOWN, upwelling longwave radiation at the earth's surface (ULRS), and GLW for each LSM are listed in Tables S16-S19. Additionally, the diurnally split surface heat flux differences for HFX, LH, and the ground fluxes (GRDFLX) are listed in Tables S20-S23. Lastly, the diurnally split surface temperature profile differences for surface skin temperature (TSK), T2, lowest model layer temperature (TATM), and the surface to lowest model layer vertical temperature gradient (TGSATM) for each LSM are listed in Tables S24-S27.**

Agricultural expansion induces annual average localized warming of ~0.1-0.2 °C using Noah-MP, CLM-D, and CLM-AF, but a localized cooling of -0.12 °C using Noah. **The cooling from**

Noah for most agricultural expansion transitions occurs in response to erroneous increases in LAI (Fig. 14) that result in erroneous daytime LH increases and evaporative cooling (Table S23). However, in the transition of evergreen broad leaf forest to mosaic cropland along the coasts of Ghana and Côte d'Ivoire the LAI transition follows the other LSMs (Fig. 14), indicating that this cooling is the result of excessive daytime average USRS increases of 37.3 W m^{-2} (Table S19) from surface albedo increases (Fig. 13). In the other LSMs, this evergreen broad leaf forest to mosaic cropland transition results in the strongest warming response from agricultural expansion, with an average 0.6 °C warming using Noah-MP and ~1.3-1.4 °C of warming using CLM-D and CLM-AF. **This warming is the result of reduced daytime evaporative cooling, as evidenced by the largest daytime LH reductions of any LULC transition (Tables S20-S22). However, this warming is somewhat indirect as the greatest T2 increases occur during the nighttime. This is because the reduced daytime LH leads to greater land surface heat storage via the GRDFLX, which is then released at night heating the atmosphere. For most other agricultural expansion transitions, CLM-AF predicts nighttime warming consistent with reduced daytime LH and increased daytime GRDFLX, as described above. The exception is the grassland to mosaic cropland transition, where most warming occurs during the daytime due to reductions in USRS from albedo increases that increase TSK and HFX warming the atmosphere (Tables S16, S20, and S24).** Noah-MP predicts less warming **with no clear signal as to the mechanism behind the warming**. This is caused by the relative insensitivity of **LH (Table S21)** to agricultural expansion **in Noah-MP**, which allows **other processes such as surface albedo changes, biogeophysical effects of RL changes (Winckler et al., 2019; Breil et al., 2020), and other secondary feedbacks to compensate each other resulting in a weaker climate signal**. The behavior of CLM-AF is consistent with the global remote sensing work of Duveiller et al. (2018), which indicates losses in latent heat flux for all natural vegetation to cropland transitions. CLM-D has many T2 changes similar to CLM-AF with some exceptions. The erroneous treatment of albedo for woody savanna in CLM-D, being too high**, leads to excessive daytime increases in USRS of 29.8 W m^{-2} (Table S18) for the transitions from woody savanna to mosaic cropland, which cools the surface (Table S26)**, reduces the **HFX (Table S22)**, and results in minor cooling. **In the other transitions from grasslands to different types of cropland, CLM-D does not have as strong a daytime LH reduction as CLM-AF, leading to either similar or weaker T2 warming that may be affected more by feedbacks from other model processes**.

Deforestation/degradation grid cells experience an average 0.22 °C warming using CLM-AF, while the remaining LSMs predict almost no change in T2 for these grid cells (e.g., -0.03 – 0.04 °C). The strong warming signal in CLM-AF **can potentially come from multiple mechanisms, but in all deforestation transitions the reduced daytime LH and increased daytime GRDFLX that leads to nighttime T2 warming appears to dominate (Tables S20 and S24). Unlike agricultural expansion, deforestation in CLM-AF causes decreases in daytime HFX. This could potentially be the result of biogeophysical effects of reduced RL making surface heating less efficient, or it may be related to the relatively larger increases in USRS from deforestation reducing energy input. In Noah-MP, smaller changes in evapotranspiration coupled with greater enhancements in surface reflectance for the woody savanna to**

savanna transition lead to little to no climate signal in T2. For the other deforestation transitions, Noah-MP predicts daytime TSK increases unlike CLM-AF (Tables S24 and S25), but little to no change in annual average T2. This may be related to the effects of RL reductions reducing daytime HFX (Table S21) and increasing TGSATM (Table 25). The reduced heating efficiency coupled with reduced available energy from either increased daytime USRS or reduced daytime SWDOWN leads to small daytime T2 cooling in these transitions that compensates any nighttime warming from reduced evapotranspiration. In CLM-D, the overall small change in annual average T2 from deforestation/degradation is due to offsetting changes in different LULC transitions. **This offsetting behavior is primarily related to the woody savanna albedo and LAI errors that when combined do not substantially reduce the daytime LH (-0.1 W m^{-2}) and excessively enhance daytime USRS (18.9 W m^{-2}) in grid cells with woody savanna to savanna transitions (Tables S22 and S26).** Since woody savanna to savanna transitions comprise a substantial portion of the total deforestation/degradation grid cells, this signal cancels the warming from other transitions. **The warming from CLM-D in the other deforestation transitions appears somewhat similar to CLM-AF. The daytime LH reduction / nighttime T2 increase mechanism appears to be responsible for the warming in the savanna to grassland transition. However, the nighttime warming in the savanna to open shrubland transition appears to be related to reduced daytime HFX that increases the daytime GRDFLX, which could be related to either reductions in USRS from albedo reductions or biogeophysical impacts from reduced RL.** Noah also experiences offsetting impacts from different deforestation/degradation transitions. Noah predicts **annual average warming for the woody savanna to savanna transitions. This is caused primarily by large daytime decreases in USRS (-35.0 W m^{-2}) and increases in HFX (23.9 W m^{-2}), which increases daytime T2 despite decreases in daytime TSK (Tables S19, S23, and S27). This suggests that the warming in this transition for Noah is primarily related to either excessive surface albedo changes or the erroneous increase in RL in this transition that increases the heating efficiency of the atmosphere.** Noah predicts cooling T2 for the other dominant deforestation/degradation transitions, **primarily due to albedo reductions that are not countered by any substantial reduction in LH**.

Grid cells that experience greening have annual average cooling using Noah-MP, CLM-D, and CLM-AF **(Table 10). CLM-AF and CLM-D predict similar cooling (-0.41°C and -0.33°C, respectively). In the transitions from barren lands to vegetation, the primary mechanism responsible for the cooling in both LSMs is enhanced daytime LH that reduces the daytime GRDFLX, which reduces nighttime heat release. In the grassland to savanna transition, the cooling for both LSMs results from reduced daytime GRDFLX that appears to be related to either other model feedbacks that reduce daytime SWDOWN or enhanced daytime HFX via the biogeophysical impacts of increased RL. In CLM-AF, the savanna to woody savanna transition experiences cooling via the increased daytime LH / nighttime cooling mechanism discussed above. However, CLM-D predicts slight annual average warming due to the erroneously large reduction in daytime USRS of -18.7 W m^{-2} (Table S18) due to the treatment of woody savanna as closed shrubland in CLM-D. This large reduction in USRS overwhelms the daytime LH increases and increases the daytime GRDFLX, causing nighttime warming. Noah-MP predicts slightly weaker annual average cooling (-0.13 °C)**

from greening. The mechanisms responsible for the cooling in Noah-MP for most transitions are similar to CLM-AF with similar daytime LH increases, except the daytime GRDFLX reductions are not as large (Tables S20-S21). However, because Noah-MP does not predict any change in LAI between savanna and woody savanna, this transition has little change in LH and a negligible change in T2. Finally, the Noah simulations continue to be an outlier with almost no change (0.02 ℃) due to offsetting inaccurate surface property changes in different greening LULC transitions."

Table S16: Annual Average Surface Radiative Flux Change (W m^{-2}) in WRF Grid Cells that experience LULCCs between 2001 and 2015 with CLM-AF

	USRS		SWDOWN		ULRS		GLW	
Transition	Day	Night	Day	Night	Day	Night	Day	Night
Agricultural Expansion*	1.6	-	0.4	-	4.0	1.0	0.0	0.2
10 to 12	2.1	-	-0.3	-	3.3	0.0	0.0	0.0
2 to 14	11.9	-	2.3	-	19.4	10.9	0.4	1.0
8 to 14	3.1	-	0.9	-	3.5	1.2	-0.1	0.3
10 to 14	-4.4	-	-2.3	-	3.4	-1.5	0.4	-0.1
Deforestation/Degradation*	7.2	-	2.4	-	1.3	2.7	-0.4	0.1
8 to 9	4.3	-	1.2	-	3.5	1.3	-0.3	0.0
9 to 7	5.9	-	2.3	-	-0.8	1.5	-0.4	0.1
9 to 10	20.0	-	7.2	-	-7.9	8.8	-1.2	0.4
Greening*	-11.1	-	-2.2	-	4.8	-6.8	-0.2	-0.6
9 to 8	-3.4	-	0.7	-	-2.6	-1.0	-0.2	-0.4
10 to 9	-0.4	-	-4.6	-	0.3	-3.4	0.8	-0.7
16 to 7	-14.7	-	-6.0	-	20.4	-8.8	-0.1	-0.7
16 to 10	-37.9	-	-7.1	-	26.5	-23.0	-0.6	-1.5

*: Shows average difference for a broad class of LULCC followed by the average difference in the major MODIS LULC transitions that comprise that class. MODIS Land Use Categories: 2 – Evergreen Broad Leaf Forest; 7 – Open Shrublands; 8 – Woody Savanna; 9 – Savannas; 10 – Grasslands; 12 – Croplands; 14 –Cropland/Natural Mosaic; 16 – Barren/ Sparsely Vegetated.

Table S17: Annual Average Surface Radiative Flux Change (W m^{-2}) in WRF Grid Cells that experience LULCCs between 2001 and 2015 with Noah-MP

	USRS		SWDOWN		ULRS		GLW	
Transition	Day	Night	Day	Night	Day	Night	Day	Night
Agricultural Expansion*	22.8	-	8.0	-	4.7	1.1	-0.9	0.0
10 to 12	-0.5	-	0.2	-	2.4	0.7	-0.1	0.1
2 to 14	25.2	-	10.6	-	13.5	6.0	-0.4	0.4
8 to 14	33.3	-	12.4	-	4.9	0.8	-1.5	-0.1
10 to 14	-0.7	-	0.4	-	0.8	0.4	-0.1	0.0
Deforestation/Degradation*	9.1	-	1.9	-	1.6	-0.1	-0.3	-0.1
8 to 9	9.7	-	2.3	-	-0.1	-0.1	-0.3	-0.1
9 to 7	-3.1	-	-2.1	-	5.6	-0.9	-0.1	-0.3
9 to 10	20.7	-	4.4	-	2.3	-0.3	-0.6	-0.1
Greening*	-6.3	-	-1.1	-	-3.7	-0.9	0.0	-0.1
9 to 8	-8.9	-	-1.9	-	-0.1	-0.1	0.1	-0.2
10 to 9	-25.2	-	-7.5	-	-3.4	-0.5	0.7	-0.4
16 to 7	-5.5	-	-1.2	-	-4.0	-0.6	0.1	0.2
16 to 10	1.6	-	0.6	-	-5.1	-1.9	-0.2	0.1

*: Shows average difference for a broad class of LULCC followed by the average difference in the major MODIS LULC transitions that comprise that class. MODIS Land Use Categories: 2 – Evergreen Broad Leaf Forest; 7 – Open Shrublands; 8 – Woody Savanna; 9 – Savannas; 10 – Grasslands; 12 – Croplands; 14 –Cropland/Natural Mosaic; 16 – Barren/ Sparsely Vegetated.

Table S18: Annual Average Surface Radiative Flux Change (W m^{-2}) in WRF Grid Cells that experience LULCCs between 2001 and 2015 with CLM-D

	USRS		SWDOWN		ULRS		GLW	
Transition	Day	Night	Day	Night	Day	Night	Day	Night
Agricultural Expansion*	17.4	-	6.2	-	-10.5	3.8	-0.6	0.3
10 to 12	3.3	-	1.4	-	-11.6	8.2	0.1	0.4
2 to 14	12.9	-	5.0	-	11.4	11.4	0.0	1.0
8 to 14	29.8	-	9.4	-	-15.8	1.3	-0.9	0.2
10 to 14	1.4	-	0.8	-	-6.0	4.1	-0.2	0.1
Deforestation/Degradation*	11.1	-	1.4	-	-2.6	-0.3	-0.1	-0.1
8 to 9	18.9	-	2.1	-	-6.4	-2.6	0.0	-0.3
9 to 7	-7.3	-	-3.1	-	2.2	3.0	-0.1	0.3
9 to 10	8.6	-	2.8	-	-2.0	2.1	-0.4	0.2
Greening*	-19.2	-	-3.3	-	7.9	-6.3	0.2	-0.4
9 to 8	-18.7	-	-2.6	-	4.9	1.4	-0.1	0.1
10 to 9	-2.8	-	-6.8	-	0.9	-4.3	1.0	-0.7
16 to 7	-37.5	-	-7.3	-	26.9	-11.6	1.0	-0.8
16 to 10	-21.2	-	-3.8	-	19.4	-20.8	0.1	-1.4

*: Shows average difference for a broad class of LULCC followed by the average difference in the major MODIS LULC transitions that comprise that class. MODIS Land Use Categories: 2 – Evergreen Broad Leaf Forest; 7 – Open Shrublands; 8 – Woody Savanna; 9 – Savannas; 10 – Grasslands; 12 – Croplands; 14 –Cropland/Natural Mosaic; 16 – Barren/ Sparsely Vegetated.

Table S19: Annual Average Surface Radiative Flux Change (W m^{-2}) in WRF Grid Cells that experience LULCCs between 2001 and 2015 with Noah

	USRS		SWDOWN		ULRS		GLW	
Transition	Day	Night	Day	Night	Day	Night	Day	Night
Agricultural Expansion*	-10.3	-	-2.2	-	0.5	-1.2	0.3	0.1
10 to 12	-3.5	-	-1.1	-	1.4	-0.2	0.1	0.1
2 to 14	37.3	-	11.9	-	-1.6	-2.0	-0.5	-0.1
8 to 14	-32.2	-	-7.6	-	-1.1	-1.9	0.7	0.3
10 to 14	-2.1	-	-1.1	-	0.8	-0.4	0.2	0.1
Deforestation/Degradation*	-12.4	-	-2.3	-	-0.4	-0.5	0.3	0.1
8 to 9	-35.0	-	-6.7	-	-1.6	-0.9	0.8	0.1
9 to 7	29.0	-	5.2	-	2.5	1.1	-0.7	0.1
9 to 10	4.0	-	0.2	-	1.1	-0.2	0.0	0.1
Greening*	-18.0	-	-2.6	-	3.7	0.4	0.3	-0.1
9 to 8	34.8	-	5.6	-	2.5	0.9	-0.4	0.2
10 to 9	-5.4	-	-1.7	-	-1.2	0.2	0.3	0.2
16 to 7	-59.2	-	-8.0	-	7.6	-0.2	0.9	-0.5
16 to 10	-82.8	-	-12.7	-	5.7	-0.7	1.4	-0.7

*: Shows average difference for a broad class of LULCC followed by the average difference in the major MODIS LULC transitions that comprise that class. MODIS Land Use Categories: 2 – Evergreen Broad Leaf Forest; 7 – Open Shrublands; 8 – Woody Savanna; 9 – Savannas; 10 – Grasslands; 12 – Croplands; 14 –Cropland/Natural Mosaic; 16 – Barren/ Sparsely Vegetated.

Table S20: Annual Average Surface Heat Flux Change (W m^{-2}) in WRF Grid Cells that experience LULCCs between 2001 and 2015 with CLM-AF

	HFX		LH		GRDFLX	
Transition	Day	Night	Day	Night	Day	Night
Agricultural Expansion*	0.6	1.2	-9.0	1.1	4.0	-3.8
10 to 12	0.9	0.4	-6.0	0.4	2.1	-2.1
2 to 14	0.4	9.7	-61.0	8.7	31.1	-30.1
8 to 14	-1.4	1.6	-8.7	0.9	3.8	-3.7
10 to 14	10.0	-1.0	-4.3	-0.4	-1.3	1.1
Deforestation/Degradation*	-6.7	2.2	-8.3	0.7	5.3	-5.1
8 to 9	-4.7	1.6	-6.4	0.4	3.7	-3.6
9 to 7	-14.7	2.6	-10.1	0.8	7.5	-7.1
9 to 10	-9.3	2.4	-4.2	0.4	4.6	-4.3
Greening*	8.4	-3.8	13.3	-1.4	-9.0	8.7
9 to 8	3.0	-1.8	7.4	-0.6	-3.4	3.2
10 to 9	13.8	-4.3	-0.1	-1.3	-9.8	8.8
16 to 7	10.0	-2.8	4.7	-0.3	-6.1	5.8
16 to 10	27.3	-3.9	10.3	-0.5	-11.9	11.8

*: Shows average difference for a broad class of LULCC followed by the average difference in the major MODIS LULC transitions that comprise that class. MODIS Land Use Categories: 2 – Evergreen Broad Leaf Forest; 7 – Open Shrublands; 8 – Woody Savanna; 9 – Savannas; 10 – Grasslands; 12 – Croplands; 14 –Cropland/Natural Mosaic; 16 – Barren/ Sparsely Vegetated.

Table S21: Annual Average Surface Heat Flux Change (W m^{-2}) in WRF Grid Cells that experience LULCCs between 2001 and 2015 with Noah-MP

	HFX		LH		GRDFLX	
Transition	Day	Night	Day	Night	Day	Night
Agricultural Expansion*	-20.1	1.9	-3.3	0.0	3.0	-2.9
10 to 12	-3.6	0.6	1.0	-0.4	0.9	-0.8
2 to 14	-4.2	6.6	-38.6	1.9	14.0	-13.8
8 to 14	-30.8	2.2	0.6	-0.1	3.0	-3.0
10 to 14	-2.1	0.2	1.8	-0.2	0.4	-0.4
Deforestation/Degradation*	-7.6	0.9	-2.3	-0.1	0.8	-0.8
8 to 9	-7.6	0.3	-0.2	0.0	0.3	-0.3
9 to 7	-2.2	1.9	-3.6	-0.1	1.1	-1.1
9 to 10	-19.1	-1.0	-0.2	1.0	1.1	-1.1
Greening*	1.5	-1.3	9.4	0.0	-2.0	2.0
9 to 8	6.5	-0.4	0.7	0.1	-0.2	0.2
10 to 9	24.6	-1.8	-0.7	0.0	-2.2	1.9
16 to 7	2.2	-0.7	7.8	0.1	-1.4	1.4
16 to 10	-2.9	-1.3	10.2	0.3	-3.1	2.9

*: Shows average difference for a broad class of LULCC followed by the average difference in the major MODIS LULC transitions that comprise that class. MODIS Land Use Categories: 2 – Evergreen Broad Leaf Forest; 7 – Open Shrublands; 8 – Woody Savanna; 9 – Savannas; 10 – Grasslands; 12 – Croplands; 14 –Cropland/Natural Mosaic; 16 – Barren/ Sparsely Vegetated.

Table S22: Annual Average Surface Heat Flux Change (W m^{-2}) in WRF Grid Cells that experience LULCCs between 2001 and 2015 with CLM-D

	HFX		LH		GRDFLX	
Transition	Day	Night	Day	Night	Day	Night
Agricultural Expansion*	-8.8	1.9	-8.1	0.2	3.9	-3.8
10 to 12	0.0	0.4	-3.1	-1.2	0.3	-0.3
2 to 14	-3.2	12.3	-63.0	6.2	31.9	-30.7
8 to 14	-12.1	0.2	-2.8	-0.5	-0.5	0.5
10 to 14	0.8	0.1	-0.5	-0.8	-0.3	0.3
Deforestation/Degradation*	-4.5	0.3	-2.9	0.0	0.3	-0.4
8 to 9	-1.9	-2.0	-0.1	-0.6	-4.7	4.4
9 to 7	-6.0	1.9	0.5	0.2	3.3	-3.3
9 to 10	-14.0	3.2	-2.3	0.2	6.0	-5.7
Greening*	7.8	-3.2	16.6	-0.7	-7.6	7.4
9 to 8	-0.7	1.6	5.1	0.8	3.8	-3.5
10 to 9	16.8	-5.0	-1.1	-1.0	-11.5	10.4
16 to 7	24.7	-4.9	13.6	0.1	-10.1	9.8
16 to 10	13.3	-4.0	17.5	-0.8	-13.7	13.5

*: Shows average difference for a broad class of LULCC followed by the average difference in the major MODIS LULC transitions that comprise that class. MODIS Land Use Categories: 2 – Evergreen Broad Leaf Forest; 7 – Open Shrublands; 8 – Woody Savanna; 9 – Savannas; 10 – Grasslands; 12 – Croplands; 14 –Cropland/Natural Mosaic; 16 – Barren/ Sparsely Vegetated.

Table S23: Annual Average Surface Heat Flux Change (W m^{-2}) in WRF Grid Cells that experience LULCCs between 2001 and 2015 with Noah

	HFX		LH		GRDFLX	
Transition	Day	Night	Day	Night	Day	Night
Agricultural Expansion*	5.4	-0.7	5.5	-1.0	3.1	-3.0
10 to 12	-0.8	0.4	2.3	-0.2	0.2	-0.2
2 to 14	-0.4	1.2	-21.2	-2.0	2.8	-2.7
8 to 14	11.9	-2.0	20.1	-1.4	5.8	-5.7
10 to 14	-2.3	0.5	3.0	-0.2	0.3	-0.3
Deforestation/Degradation*	9.3	-1.1	3.7	-0.5	2.2	-2.2
8 to 9	23.9	-2.9	11.4	-0.8	4.7	-4.6
9 to 7	-23.2	2.8	-7.8	0.2	-4.0	3.9
9 to 10	-3.8	-0.1	-0.2	-0.4	0.8	-0.8
Greening*	12.2	-1.0	0.0	0.2	0.2	-0.3
9 to 8	-16.6	2.8	-19.7	0.7	-4.3	4.2
10 to 9	6.2	0.1	-1.7	0.4	-0.7	0.6
16 to 7	42.5	-3.4	5.9	-0.6	3.8	-3.9
16 to 10	57.6	-7.8	16.6	-0.4	8.2	-8.3

*: Shows average difference for a broad class of LULCC followed by the average difference in the major MODIS LULC transitions that comprise that class. MODIS Land Use Categories: 2 – Evergreen Broad Leaf Forest; 7 – Open Shrublands; 8 – Woody Savanna; 9 – Savannas; 10 – Grasslands; 12 – Croplands; 14 –Cropland/Natural Mosaic; 16 – Barren/ Sparsely Vegetated.

Table S24: Annual Average Near Surface Temperature Profile Change in WRF Grid Cells that experience LULCCs between 2001 and 2015 with CLM-AF

	TSK (°C)		T2 (°C)		TATM (10^{-1} °C)		TGSATM (10^{-2} °C m^{-1})	
Transition	Day	Night	Day	Night	Day	Night	Day	Night
Agricultural Expansion*	0.7	0.1	0.0	0.3	0.1	0.7	2.2	0.0
10 to 12	0.7	0.0	0.1	0.2	0.2	0.2	2.1	-0.3
2 to 14	3.1	1.8	0.4	2.3	1.8	6.3	9.6	2.0
8 to 14	0.5	0.2	0.0	0.3	-0.1	0.5	1.8	0.3
10 to 14	0.8	-0.3	0.1	0.0	0.7	-0.2	2.5	-0.9
Deforestation/Degradation*	0.0	0.5	0.0	0.4	-0.2	1.4	0.2	0.8
8 to 9	0.5	0.2	0.0	0.3	-0.2	0.8	1.9	0.1
9 to 7	-1.9	1.9	-0.1	0.8	-0.2	4.0	-6.4	4.0
9 to 10	-0.4	0.3	-0.1	0.3	-0.7	0.7	-1.1	0.5
Greening*	1.1	-1.4	-0.1	-0.7	-1.3	-2.5	4.6	-3.1
9 to 8	-0.4	-0.2	0.0	-0.2	0.2	-0.4	-1.5	-0.2
10 to 9	0.5	-0.6	0.1	-0.6	0.7	-2.5	1.4	-0.3
16 to 7	4.0	-2.0	-0.3	-0.5	-3.7	-2.9	16.2	-5.0
16 to 10	4.8	-4.8	-0.1	-1.4	-2.8	-6.1	17.8	-12.4

*: Shows average difference for a broad class of LULCC followed by the average difference in the major MODIS LULC transitions that comprise that class. MODIS Land Use Categories: 2 – Evergreen Broad Leaf Forest; 7 – Open Shrublands; 8 – Woody Savanna; 9 – Savannas; 10 – Grasslands; 12 – Croplands; 14 –Cropland/Natural Mosaic; 16 – Barren/ Sparsely Vegetated.

Table S25: Annual Average Near Surface Temperature Profile Change in WRF Grid Cells that experience LULCCs between 2001 and 2015 with Noah-MP

	TSK (°C)		T2 (°C)		TATM (10^{-1} °C)		TGSATM (10^{-2} °C m^{-1})	
Transition	Day	Night	Day	Night	Day	Night	Day	Night
Agricultural Expansion*	0.7	0.2	0.0	0.2	-1.3	0.9	3.3	0.1
10 to 12	0.4	0.1	0.2	0.1	0.0	0.7	1.4	0.1
2 to 14	2.2	1.0	0.3	0.9	0.5	4.1	7.4	0.8
8 to 14	0.8	0.1	-0.2	0.2	-2.2	0.5	3.9	0.1
10 to 14	0.1	0.1	0.1	0.1	-0.1	0.2	0.5	0.1
Deforestation/Degradation*	0.3	0.0	-0.1	0.0	-0.6	-0.1	1.3	0.0
8 to 9	0.0	0.0	-0.1	0.0	-0.6	-0.1	0.3	0.0
9 to 7	0.9	-0.1	-0.2	0.1	-0.5	-0.5	3.3	-0.2
9 to 10	0.3	-0.1	-0.1	0.0	-1.2	-0.1	1.9	-0.1
Greening*	-0.6	-0.2	-0.1	-0.2	-0.1	-0.1	-2.0	-0.5
9 to 8	0.0	0.0	0.0	0.0	0.3	-0.1	-0.2	0.1
10 to 9	-0.5	-0.1	0.2	-0.2	0.1	-0.1	-2.6	0.2
16 to 7	-0.6	-0.1	-0.1	-0.1	-0.1	0.9	-2.2	-1.1
16 to 10	-0.8	-0.3	-0.1	-0.3	-0.4	0.8	-2.5	-1.7

*: Shows average difference for a broad class of LULCC followed by the average difference in the major MODIS LULC transitions that comprise that class. MODIS Land Use Categories: 2 – Evergreen Broad Leaf Forest; 7 – Open Shrublands; 8 – Woody Savanna; 9 – Savannas; 10 – Grasslands; 12 – Croplands; 14 –Cropland/Natural Mosaic; 16 – Barren/ Sparsely Vegetated.

Table S26: Annual Average Near Surface Temperature Profile Change in WRF Grid Cells that experience LULCCs between 2001 and 2015 with CLM-D

	TSK (°C)		T2 (°C)		TATM (10^{-1} °C)		TGSATM (10^{-2} °C m^{-1})	
Transition	Day	Night	Day	Night	Day	Night	Day	Night
Agricultural Expansion*	-2.0	0.8	-0.1	0.3	-0.5	1.5	-6.6	1.7
10 to 12	-2.4	1.8	0.1	0.2	1.6	2.4	-9.3	4.7
2 to 14	1.3	1.9	0.4	2.3	1.2	6.4	3.9	2.3
8 to 14	-2.7	0.3	-0.2	-0.1	-1.3	0.3	-8.3	0.8
10 to 14	-1.3	0.9	0.0	0.1	-0.1	0.8	-4.3	2.7
Deforestation/Degradation*	-0.4	-0.1	0.0	0.0	-0.3	-0.2	-1.0	-0.1
8 to 9	-0.7	-0.5	0.0	-0.4	-0.2	-1.3	-2.3	-0.7
9 to 7	0.0	0.6	-0.1	0.4	-1.3	0.9	0.8	1.5
9 to 10	-0.6	0.3	-0.1	0.3	-1.1	0.9	-1.5	0.6
Greening*	1.6	-1.3	0.0	-0.6	-0.2	-2.6	5.4	-2.7
9 to 8	0.5	0.3	0.0	0.2	-0.5	0.1	2.1	0.7
10 to 9	0.7	-0.7	0.1	-0.7	0.9	-2.9	1.7	-0.5
16 to 7	5.3	-2.5	0.2	-0.9	0.8	-0.4	17.4	-6.1
16 to 10	3.6	-4.2	0.0	-1.6	-0.4	-5.6	12.3	-10.8

*: Shows average difference for a broad class of LULCC followed by the average difference in the major MODIS LULC transitions that comprise that class. MODIS Land Use Categories: 2 – Evergreen Broad Leaf Forest; 7 – Open Shrublands; 8 – Woody Savanna; 9 – Savannas; 10 – Grasslands; 12 – Croplands; 14 –Cropland/Natural Mosaic; 16 – Barren/ Sparsely Vegetated.

Table S27: Annual Average Near Surface Temperature Profile Change in WRF Grid Cells that experience LULCCs between 2001 and 2015 with Noah

	TSK (°C)		T2 (°C)		TATM (10^{-1} °C)		TGSATM (10^{-2} °C m^{-1})	
Transition	Day	Night	Day	Night	Day	Night	Day	Night
Agricultural Expansion*	-0.2	-0.4	0.1	-0.3	0.1	-1.1	-0.7	-0.5
10 to 12	0.1	-0.1	-0.1	-0.1	-0.1	-0.1	0.3	-0.4
2 to 14	-0.3	-0.4	-0.3	-0.3	-0.2	-0.7	-0.7	-0.8
8 to 14	-0.5	-0.5	0.3	-0.5	0.3	-2.0	-1.9	-0.4
10 to 14	0.0	-0.2	-0.1	-0.1	-0.2	-0.1	0.1	-0.5
Deforestation/Degradation*	-0.1	-0.1	0.2	-0.1	0.5	-0.3	-0.6	-0.1
8 to 9	-0.1	-0.1	0.5	-0.1	1.2	-0.8	-1.2	0.3
9 to 7	0.1	0.0	-0.5	0.1	-0.8	1.2	0.9	-0.7
9 to 10	-0.1	-0.2	-0.1	-0.1	-0.3	-0.3	-0.2	-0.4
Greening*	0.3	-0.1	0.2	-0.1	0.9	-0.5	0.4	-0.1
9 to 8	0.3	0.1	-0.3	0.1	-0.6	0.6	1.4	-0.2
10 to 9	0.2	0.3	0.1	0.2	0.4	0.9	0.4	0.3
16 to 7	0.5	-0.5	0.5	-0.5	2.6	-1.7	0.0	-0.7
16 to 10	0.2	-0.5	0.8	-0.6	3.1	-3.1	-1.3	0.2

*: Shows average difference for a broad class of LULCC followed by the average difference in the major MODIS LULC transitions that comprise that class. MODIS Land Use Categories: 2 – Evergreen Broad Leaf Forest; 7 – Open Shrublands; 8 – Woody Savanna; 9 – Savannas; 10 – Grasslands; 12 – Croplands; 14 –Cropland/Natural Mosaic; 16 – Barren/ Sparsely Vegetated.

2) simulation results show that the cloud cover is consistently overestimated in the validation experiment. At the same time, downward short-wave radiation (swdown?) is also overestimated. How does that fit together?

Response: We thank the reviewer for their comment. The cloud fraction (i.e. cloud cover) parameter only refers to the spatial extent of clouds, while the swdown parameter is determined by the cloud's optical thickness. For example, a model grid column that contains a single high-level cirrus cloud would have a cloud fraction of 100%, but that cloud would be very thin and not drastically reduce the swdown parameter. In these simulations, it is likely that the model is producing excess anvil clouds from the convection, resulting in the overpredicted cloud fraction. However, the clouds that do exist in the model are not sufficiently optically thick enough to reduce the swdown to the appropriate level. This can be seen in Figure S6 of the updated supplementary material, where the shortwave and longwave cloud forcing are underpredicted in all model configurations.

We have added the following sentence to the discussion of radiation variables for clarity:

Lines 465-467 revised manuscript: "**The underestimated cloud radiative forcing seems to indicate the model is not generating clouds of sufficient optical thickness, since cloud fractions are overestimated compared to satellite estimates (Fig. 10, Fig. S15).**"

3) Several abbreviations are used which are not explained in the text (e.g. SWDOWN, GLW, OLR, SWUPT).

Response: We thank the reviewer for their comment and bringing this to our attention. We found some inconsistencies in the names between the tables, supplementary material, and the main text. We have updated Table 9 below for consistency and added the full names in the main text before any abbreviations used.

Table 9: Evaluated Variables and Evaluation Datasets

Variable	Acronym	Evaluation Dataset
2-m Temperature	T2	CRU TS4.02 and NCDC-ISD
Daily Maximum Temperature	T2MAX	CRU TS4.02
Daily Minimum Temperature	T2MIN	CRU TS4.02
Diurnal Temperature Range	DTR	CRU TS4.02
2-m Vapor Pressure	E2	CRU TS4.02
2-m Dew point Temperature	T_d2	NCDC-ISD
Precipitable Water Vapor	PWV	MOD08_M3
Cloud Fraction	CF	CRU TS4.02 and MOD08_M3
Precipitation	PRE	CRU TS4.02, GPCP, and TRMM
10 m Wind Speed	WSP10	NCDC-ISD
Downwelling Shortwave Radiation (Surface)	SWDOWN	CERES-EBAF
Downwelling Longwave Radiation (Surface)	GLW	CERES-EBAF
Upwelling Shortwave Radiation (TOA*)	SWUPT	CERES-EBAF
Upwelling Shortwave Radiation (Surface)	USRS	CERES-EBAF
Upwelling Longwave Radiation (TOA*)	OLR	CERES-EBAF
Shortwave Cloud Forcing	SWCF	CERES-EBAF
Longwave Cloud Forcing	LWCF	CERES-EBAF

*: Top of the Atmosphere

References:

Breil, M., and Coauthors, (2020). The Opposing Effects of Reforestation and Afforestation on the Diurnal Temperature Cycle at the Surface and in the Lowest Atmospheric Model Level in the European Summer. *Journal of Climate*, *33*(21), 9159-9179.

Winckler, J., and Coauthors, 2019: Different response of surface temperature and air temperature todeforestation in climate models. Earth Syst. Dyn., 10, 473–484, https://doi.org/10.5194/esd-10-473-2019.